Research paper

Preparation and Characterization of Nanocrystalline Cellulose by Acid Hydrolysis of Cotton Linter

Chih-Ping Chang,[1] I-Chen Wang,[2] Kuo-Jung Hung,[1] Yuan-Shing Perng[3,4]

【Summary】

The purpose of this study was to use acid hydrolysis of cotton linter to generate nanocrystalline cellulose (NCC). Based on a 2^4 factorial design, the effects of sulfuric acid concentration, temperature, hydrolysis time, and the solid/liquid ratio on the NCC yield were examined. NCC specimens obtained from different sulfuric acid concentrations were subjected to a battery of analyses, including dynamic light scattering (DLS), transmission electron microscopy (TEM), Fourier-transform infrared spectroscopy (FTIR), ^{13}C solid-state nuclear magnetic resonance (^{13}CSNMR), and a thermal gravimetric analysis (TGA) to probe the particle size distribution, morphology, functional group shifts, position of the carbon, and thermal degradation properties of the ensuing NCC. The results indicated that the sulfuric acid concentration and solid/liquid ratio at higher levels, and temperature and reaction time at lower levels were significantly conducive to increases in NCC yields. The main effects in diminishing order were the acid concentration, temperature, hydrolysis time, and solid/liquid ratio. Results of DLS and TEM observations suggested that the NCC had a size distribution centered around 20~200 nm, with length-to-width ratios ranging 1:1~1:30. The FTIR analysis indicated that absorption peaks at 1010~1080 and 1150~1260 cm^{-1} were derived from sulfate ester bonds on the cellulosic chains. Solid state ^{13}CNMR spectra indicated that the C4 atoms along the cellulosic chain were shifted from 87.4 ppm to a lower magnetic domain, indicating the sulfonic ester bonding position. The TGA indicated that the lower-sulfuric-acid NCC specimen began step 1 weight loss at ca. 149℃, whereas its starting temperature of step 2 weight loss was generally higher than the mid- and high-acid NCC, at 337 and 205℃, respectively. The high-acid NCC only showed marked weight loss at 243℃. The study found that a sulfuric acid concentration of 60%, a solid/liquid ratio of 1:20, a hydrolysis temperature of 45℃, and a hydrolysis time of 5 min produced the best yield of 54.4%.

Key words: cotton linter, nanocrystalline cellulose, sulfuric acid hydrolysis, ^{13}C solid state nuclear magnetic resonance, thermo-gravimetric analysis.

Chang CP, Wang IC, Hung KJ, Perng YS. 2010. Preparation and characterization of nanocrystalline cellulose by acid hydrolysis of cotton linter. Taiwan J For Sci 25(3):251-64.

[1] Department of Forestry, National Chung Hsing University, 250 Guoguang Rd., Taichung 40227, Taiwan. 國立中興大學森林學系，40227台中市國光路250號。

[2] Wood Cellulose Division, Taiwan Forestry Research Institute, 53 Nanhai Rd., Taipei 10066, Taiwan. 林業試驗所木材纖維組，10066台北市南海路53號。

[3] Department of Environmental Engineering, Da-Yeh University, 168 Xuefu Rd., Dacun Township, Changhua 51591, Taiwan. 大葉大學環境工程學系，51591彰化縣大村鄉學府路168號。

[4] Corresponding author, e-mail:ysperng@mail.dyu.edu.tw 通訊作者。

Received April 2010, Accepted June 2010. 2010年4月送審 2010年6月通過。

研究報告

棉漿酸水解法製備奈米纖維素及性質分析

章之平[1)] 王益真[2)] 洪國榮[1)] 彭元興[3,4)]

摘 要

本研究目的為棉漿應用硫酸水解法製備奈米纖維素，藉由2^4因子設計探討硫酸濃度、溫度、水解時間、固液比等因子對於得率的影響。不同硫酸濃度下所製得的奈米纖維素產物利用DLS、TEM、FTIR、^{13}CSNMR、TGA等儀器進行檢測，以探討奈米纖維素的粒徑分布、形態、官能基轉移、碳位置及熱分解等性質。研究結果顯示，硫酸濃度與固液比在高水準時，及溫度與時間在低水準時，對奈米纖維素產量有顯著影響。主效應依序為硫酸濃度＞溫度＞水解時間＞固液比。雷射粒徑分析儀與穿透式電子顯微鏡觀測結果顯示，實驗製得的NCC尺寸分佈集中於20~200 nm之間，長寬比由1:1~1:30不等。傅立葉轉換式紅外線光譜分析指出，在1010~1080與1150~1260 cm^{-1}處吸收峰增強，顯示纖維素長鏈上新增硫酸酯類鍵結。^{13}C固態核磁共振圖譜指出，C4位置由87.4往低磁場區移動，顯示硫酸酯類鍵結於該位置。熱重分析結果顯示，低硫酸組奈米纖維素均在149℃左右產生第一階段重量損失，第二階段熱重損失溫度低硫酸組較中高硫酸組為高，分別是337與205℃；高硫酸組僅於243℃時產生明顯的熱重損失。本研究以酸濃度60%、固液比1:20、反應溫度45℃、水解5 min所得之收率最佳，產率為54.4%。

關鍵詞：棉漿、奈米纖維素、硫酸水解、^{13}C固態核磁共振、熱重分析。

章之平、王益真、洪國榮、彭元興。2010。棉漿酸水解法製備奈米纖維素及性質分析。台灣林業科學 25(3):251-64。

INTRODUCTION

Cellulose is one of the major plant cell-wall components with an annual yield of about 1×10^{11} tons in nature. It has several valuable attributes such as being renewable, biodegradable, environmentally friendly, inexpensive, and possessing great mechanical strength; in today's world, such attributes are increasingly appreciated and of interest. Through sulfuric acid hydrolysis, a cellulosic material can easily be degraded into crystallites on the nanometer scale which are summarily named cellulose nano-crystallites (CNCs) or nanocrystalline cellulose (NCC), the latter term is used throughout this paper. The much-enhanced surface area of NCC not only helps it combine with other materials to create composite materials but also provides appropriate mechanical reinforcement. Functional groups along the NCC molecular chains can be modified to render NCC suitable for use as functional fillers and applicable to combine with medicines as slow-release tablets (Kao and Lee 2009, Stenius and Andresen 2009).

Since the 1930s, much research has focused on the sulfuric acid hydrolysis of cellulose. Materials used by researchers were mostly wood pulps, cotton linter, or various cellulosic tissues such as sisal fibers, husk fibers, barley straw, bamboo pulp, and even bacterial cellulose (Vandyke et al. 1931, Lin et al. 1991, Sun et al. 2005, Yang et al. 2008,

Wong et al. 2009, Kim et al. 2010). Some of those studies provided useful data on reaction conditions, particle size distributions, influence of sulfonic groups, and morphologies. But very few of the studies discussed the effects of individual reaction factors and correlations among them. Due to a lack of exhaustive instrumental analyses, earlier studies often evaluated a limited number of NCC characteristics, such as functional group changes and morphology, without comparisons of different results based on accurate instrumental analyses (Xiang et al. 2003, Ago et al. 2004, Zhao et al. 2006). Recent studies indicated that after sulfuric acid hydrolysis, the thermo-degradation behaviors of NCC could be significantly influenced by sulfonic esters loaded on the cellulose long chain (Wang et al. 2007, Morán et al. 2008, Zhang et al. 2008, Rosa et al. 2010, Zhang et al. 2010).

In this study, cotton linter was hydrolyzed with sulfuric acid using a 2^4 factorial design. NCC yields were used as the dependent variable in an analysis of variance (ANOVA) test, and the influences of different factors (acid concentration, solid/liquid ratio, reaction temperature, and reaction time) were examined. The NCC preparations thus obtained were then analyzed using dynamic light scattering (DLS), transmission electron microscopy (TEM), Fourier-transform infrared spectroscopy (FTIR), ^{13}C solid state nuclear magnetic resonance (^{13}CSNMR), and a thermo-gravimetric analysis (TGA). The size distribution, morphology, functional group changes, carbon atom positions, and thermal behaviors of the NCCs were evaluated.

METERIALS AND METHODS

Experimental design

All experimental processes were fitted to a 2^4 factorial design. Four independent variables were selected, each with 2 levels of variation which were determined from preliminary studies. These were sulfuric acid concentrations of 50 and 60% (A); solid/liquid ratios of 1:10 and 1:20 (B); reaction temperatures of 45 and 55℃ (C), and hydrolysis times of 5 and 15 min (D). Mid-point conditions were run with 3 replications to check the linearity of the responses. The sample matrix is shown in Table 1.

NCC yields were used as the dependent variable in ANOVA statistical test to determine the significance of the main effect of each independent variable. The most influential main effect was then chosen as a differentiating factor for subsequent instrumental characterization of the resulting NCC specimens and to provide insights into the detailed hydrolysis processes. The NCC properties investigated included the sample particle size distribution, morphology, aspect ratio, functional group changes, positions of the carbon atoms along the cellulose chain, the thermo-degradation, etc. Based on the evaluation results, the most-probable hypothesis of the sulfuric hydrolysis of cellulose was provided.

Materials

The materials used in the study, including linter and chemicals are as follows. Cotton linter with an average length of 2270.6 μm, average diameter of 26.3 μm, and average aspect ratio of 151.9 was purchased from Chung-Rhy Specialty Paper Co. (Puli, Taiwan), and 98% sulfuric acid and sodium hydroxide for pH adjustment were from AR, Panreac Quimica S.A.U. (Barcelona, Spain). To prevent fallen dust from the environment from affecting the accuracy of the NCC yields, all the liquids were first passed through a 0.45-μm-pore Teflon filter paper (Advavtec, Osaka, Japan). Dialysis tubing with a molecular weight cut off (MWCO) of 8~10 kDa was

Table 1. Factorial experimental design for 4 variables at 2 levels (2^4)

A	B	C	D	Yield (%)
Acid concentration (%)	Solid/liquid ratio	Reaction temp (℃)	Reaction time (min)	
50	10	45	5	1.6
60	10	45	5	33.2
50	20	45	5	1.8
60	20	45	5	54.5
50	10	55	5	2.0
60	10	55	5	7.3
50	20	55	5	1.9
60	20	55	5	11.6
50	10	45	15	2.2
60	10	45	15	13.5
50	20	45	15	3.5
60	20	45	15	18.2
50	10	55	15	0.6
60	10	55	15	2.2
50	20	55	15	1.0
60	20	55	15	6.7
55	15	50	10	19.5
55	15	50	10	19.1
55	15	50	10	17.5

chosen to remove extra sulfuric acid from the liquid phase (Spectra/Por 132700, Spectrum Laboratories, Houston, TX, USA).

Analytical instruments

To measure the particle size distribution of NCC samples, a dynamic light scattering meter was used (DLS Nano S90, Malvern, UK). To observe the actual sizes of the hydrolysis products, both a transmission electron microscope (JEM-1400, Jeol, Tokyo, Japan) and an optical microscope (BX 51 Olympus, Kanazawa, Japan) were used. The latter was paired with a digital video camera (SSC-DC50A Sony, Tokyo, Japan) and an Image-M measuring program (Apisc, Tao-Yuan, Taiwan). Functional group changes of the NCC samples were analyzed with a Fourier-transform IR spectrophotometer (Spectrum 100, Perkin Elmer, Waltham, MA, USA). Cross-polarization/magic angle spinning ^{13}C solid-state nuclear magnetic resonance spectroscopy in conjunction with a 5-mm PFG Triple ^{1}H-^{13}C-^{15}N resonance probe (CP/MAS $^{13}CSNMR$, Unity Inova-500, Varian, Lexington, MA, USA) analyses were performed to confirm crystalline-type changes. Thermal degradation behaviors of the NCC specimens were investigated using a thermal gravimetric analysis unit (Pyris 1, Perkin Elmer).

Methods

Before acid hydrolysis, the cotton linter was oven-dried and accurately weighed into 10-g specimens and then hydrolyzed under different conditions (cf. the 2^4 design) with continuous stirring at 400 rpm. Reactions were terminated by adding deionized water and cooling the system down to 10℃. All of the post-reaction liquid was then centrifuged

for 10 min at 10,000 rpm. The upper phase was adjusted to pH 7 by adding 1% NaOH, and then dialyzed for 72 h. All of the liquid samples were freeze-dried, and the yields calculated. All experiments were repeated in triplicate. Since the sulfuric acid concentration showed the greatest hydrolysis effect, the products of the highest yield conditions at different acid concentrations were chosen for further analyses. These samples were designated as follows: NCC50 from a 50% acid concentration, 1:20 solid/liquid ratio, 45℃ reaction temperature, and 15 min hydrolysis time; NCC55 from a 55% acid concentration, 1:15 solid/liquid ratio, 50℃ reaction temperature, and a hydrolysis time of 10 min; and NCC60 from a 60% acid concentration, 1:20 solid/liquid ratio, 45℃ reaction temperature, and a hydrolysis time of 5 min. In order to better understand the hydrolysis process at a 50% acid concentration, solid residues left after centrifuging from the NCC50 preparation were also selected and designated RS50.

For the particle size distribution measurements, all NCC samples were adjusted to a 10% concentration with deionized water and then directly observed with a DLS. The actual sizes of NCC50, NCC55, and NCC60 were observed using a TEM. The RS50 and unaltered cotton linter were observed by optical microscopy. TEM samples were adjusted to a 5% concentration with 75% ethanol, negatively stained with a 2% uranyl zinc acetate solution, and dried on carbon-coated Lacey TEM grids followed by observation. The intensity of the electron beams used was 120 kV. Samples for optical microscopic observations were adjusted to a 5% concentration before observation. From each sample, 200 particles or fibers were selected and measured to determine the average length, diameter, and aspect ratio.

The freeze-dried NCC samples were well-mixed with KBr powder and examined with an FTIR unit based on a diffuse reflectance principle. For the ^{13}CSNMR analysis, experiments were performed under a static field strength of 11.7 Tesla at 25℃, with a spin rate of 10 kHz, a delay time of 2 s, and a contact time with the cross-polarized beam of 5 ms. Moreover, the thermal degradation behaviors of the NCCs were carried out with a 10℃ min^{-1} heating rate, and a temperature range of 50~800℃, in a nitrogen atmosphere with gas flow rate of 20 ml min^{-1}.

RESULTS AND DISCUSSION

In this study, only those hydrolysis products with nano-scale sizes and certain residues were chosen as the targets of study, as other byproducts were mostly eliminated by dialysis and centrifugation. Based on the research results, we managed to delineate the main effect of each independent variable and provide on explanation for the correlations between the sulfonic esters and thermal degradation of NCCs. We also provide a hypothetical pathway of sulfuric acid hydrolysis.

Results of the 2^4 factorial design

The dependent variable (NCC yield) data listed in Table 1 were statistically tested by ANOVA. The main effects and interactions on NCCs yields as well as their statistical significances as represented by *F*-values are shown in Table 2. The 4-way ANOVA results show that the acid concentration, solid/liquid ratio, reaction temperature, and reaction time all significantly affected the NCC yield, with a significance level of $\alpha < 0.05$. The influences of the 4 factors on the total NCC yields become more significant when the acid concentration and solid/liquid ratio approached the higher level, or the reaction temperature and reaction time shifted to the lower level.

Table 2. Main effects, interactions, and *F*-values of the analysis of variance (ANOVA). In the Table, A is the sulfuric acid concentration, B is the solid/liquid ratio, C is the reaction temperature, and D is the reaction time

ANOVA	Main effect			
	A	B	C	D
Yield	16.8	4.4	11.7	8.1
F-value	3482.1	238.6	1700.8	807.7

ANOVA	Interaction										
	AB	AC	AD	BC	BD	CD	ABC	ABD	ACD	BCD	ABCD
Yield	21.2	28.5	24.8	16.1	12.5	19.8	35.1	31.7	43.1	26.0	54.0
F-value	192.7	1450.5	809.3	75.5	50.6	359.4	59.0	75.2	525.8	42.2	49.9

$F_{0.05,1,32} = 250$. For values smaller than this, the effect was not significant.

The main effects of the factors in descending order of significance were: acid concentration (A) > reaction temperature (C) > reaction time (D) > solid/liquid ratio (B). The *F* value of A was 3482.1, B was 238.6, C was 1700.8, and D was 807.7. According to the experimental design, the *F* test value of significance was $F_{0.05,1,32} = 250$; hence, factor B, the solid/liquid ratio of our choice had no significant influence on the outcome of hydrolysis.

The *F* value of all interactions showed a significant influence on hydrolysis as follow: AC = 1450.5, AD = 809.3, CD = 359.4, and ACD = 525.8. According to the *F* values obtained from the ANOVA test, the conditions with the highest yield rates under different acid concentration were chosen for further analysis. The best NCC yield obtained (54.4%) was with an acid concentration of 60%, a solid/liquid ratio of 1:20, a reaction temperature of 45℃, and a reaction time of 5 min.

Morphology and size distribution of the NCC specimens

The results of the NCC size assessment produced from the DLS, TEM, and OP techniques were compared to explain why NCC specimens had different sizes based on different measurements. Results of DLS are shown in Fig. 1. Figure 1a shows that NCC50 had sizes distributed at 91~295 nm, with an average size of 289.2 nm; Fig. 1b indicates that NCC55 had sizes distributed at 164~615 nm, with an average size of 449.4 nm. NCC60 showed a bimodal size distribution (Fig. 1c); the first peak was between 50 and 120 nm, the second peak was between 140 and 530 nm, with an average size of 319.0 nm. Measurements of the particle size distribution by DLS followed several steps. First, the time difference characteristic of each sample determined by the instrument was transformed into a correlation function through a correlator unit. Then the correlation function was applied to the velocities of particles moving in the liquid to give an equivalent spherical particle of the same velocities. The diameters of the spheres were regarded as the estimated diameters of the sample particles. Finally, the Stokes-Einstein equation was applied to calculate the thickness of the liquid surrounding the sample particles, and obtain the actual particle size by deducing the liquid film thickness from the estimated diameters. The following are equations involved in the DLS particle size estimation. Equations used for calculation are listed as follows:

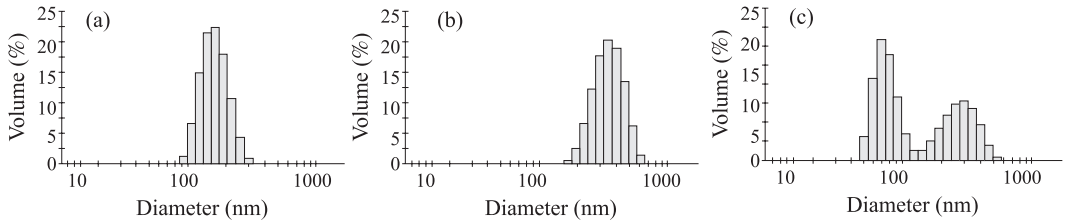

Fig. 1. Dynamic light scattering (DLS) analysis results of the acid hydrolysis products: (a) NCC50, (b) NCC55, and (c) NCC60.

(a) Correlation function of polydispersed particles

$G(\tau) = A [1 + Bg_1(\tau)^2]$;

where A is the baseline of the correlation function, B is the intercept of the correlation function, τ is the time difference of the sample recorded by a correlator, and $g_1(\tau)$ is the sum of all exponential decays contained in the correlation function.

(b) Stokes-Einstein formula

$$d_h = \frac{k_B T}{3\pi\eta_o D}$$

where d_h is the hydro-diameter, k_B is the Boltzmann constant, T is the temperature, η_o is the sample viscosity and D is a diffusion coefficient.

All of the NCC preparations showed a relatively narrow range for the size distribution, suggesting that the byproducts of hydrolysis were probably effectively removed. However, as the NCC preperations were not ideal spheres, the DLS measurements probably tended to overestimate the actual sample particle sizes.

Table 3 and Fig. 2. show the results of TEM and OP observations. As shown in Table 3, the observed sizes of NCC specimens by the TEM method were generally smaller than those obtained by the DLS method. Diameters of the hydrolyzed cellulosic materials are necessarily smaller as the outer and amorphous portions are eroded by the acid. The small size of NCC50 may have been the result of the weaker acid only partially dissolving the amorphous region on the cotton fibers. The observation of RS50 showed that the fibers retained their macroscopic shape even after 15 min of reaction time. Figure 2a shows that NCC50 had a rough surface which may have been caused by fragments aggregating into clusters leading the DLC reading to overestimate the size distribution.

Functional groups

In this study, changes in functional groups were followed using a reflectance mode of the FTIR. At the same mass basis, the cotton linter and RS50 possessed a smaller specific surface area. Thus, upon mixing with KBr, they provided smeller surfaces to be irradiated with IR than did NCC. As a consequence, cotton linter and RS50 samples produced a weaker signal than did NCC. Figure 3 shows the FTIR spectra of NCC specimens and the original cotton linter. The RS50 showed no appreciable functional group change from cotton linter, except for the 1200 cm^{-1} peak as $-SO_3$ asymmetrical stretching and a slight strengthening of the 3300 cm^{-1} hydroxyl groups. Whereas for NCC50, 55, and 60, there were all strong new peaks at 1010~1080 and 1150~1260 cm^{-1}, both of which resulted from the fresh presence of sulfate ester bonds. Upon neutralization with the NaOH solution, all of the sulfate esters should have been transformed into monoso-

Table 3. Dimensions of the hydrolysis products obtained from TEM and optical microscopy

Sample	Average length (nm)	Average diameter (nm)	Average aspect ratio
Cotton linter[a)]	227.1×10^4	2.6×10^4	151.9
RS50[a)]	138.7×10^4	1.6×10^4	65.4
NCC50	20.0	20.7	1.0
NCC55	200.3	16.3	34.0
NCC60	100.6	12.5	7.8

[a)] Samples observed by optical microscopy.

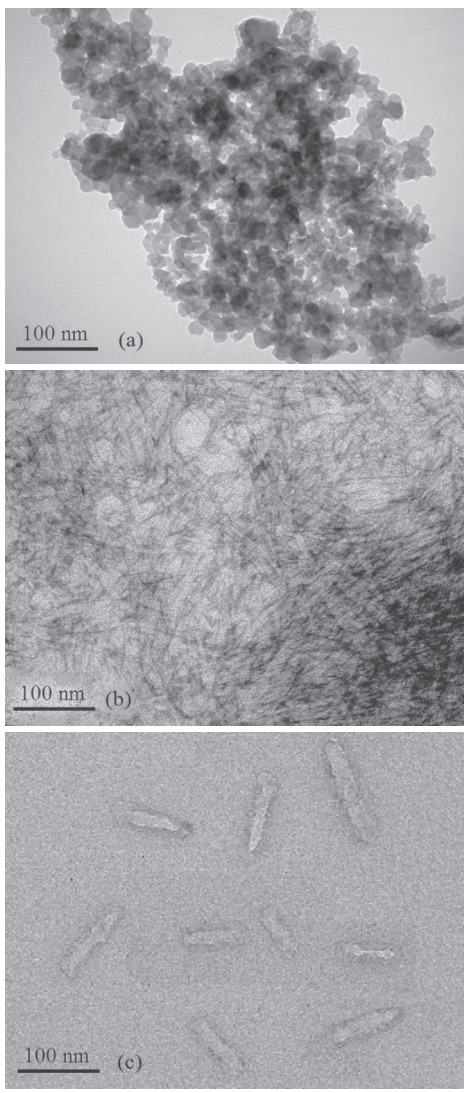

Fig. 2. TEM micrographs showing the morphology of NCC specimens produced from different hydrolysis conditions: (a) NCC50, (b) NCC55, and (c) NCC60.

dium cellulose sulfate esters, and with typical peaks at 1210, 1250, and 1080 cm^{-1}. The reason that the peak surfaces of NCC 50, 55, and 60 were larger then those of RS50 may have been due to the primary and secondary alcohols also formed during NaOH neutralization. The peaks at 2900, 1069, 1033, and 897 cm^{-1} were all typical absorption peaks of cellulosic materials, representing C-H stretching, C-O stretching, C-C skeletal vibrations, and C_1-H ring stretching of the glucose unit, respectively. The peak at 1646 cm^{-1}, however, was assigned to the -OH groups from atmospheric water vapor adsorbed onto NCC surfaces (Sun et al. 2005, Yang et al. 2008, Rosa et al. 2010).

According to a recent study (Rosa et al. 2010), the peak at 897 cm^{-1} can be used as a benchmark to identify glycoside linkage deformations among the glucose units in cellulose. Moreover, the increase in absorbance at around 3200~3600 cm^{-1} was evidently due to increases in hydroxyl groups on NCC after acid hydrolysis. However, the hydroxyl groups may also have arisen from adsorbed atmospheric moisture.

The NMR spectra showing the carbon positions on the samples are shown in Fig. 4. The relative chemical shift, δ, of the cotton linter was C1: 105.0, C2: 72.3, C3, 5: 75.4, C4: 87.4, and C6: 65.3. For RS50, these were C1: 104.5, C2: 71.5, C3, 5: 75.49, C4: 87.4, and C6: 65.3. For NCC50, these were C1: 104.9, C2, 3, and 5: 74.5, C4: 89.2, and C6:

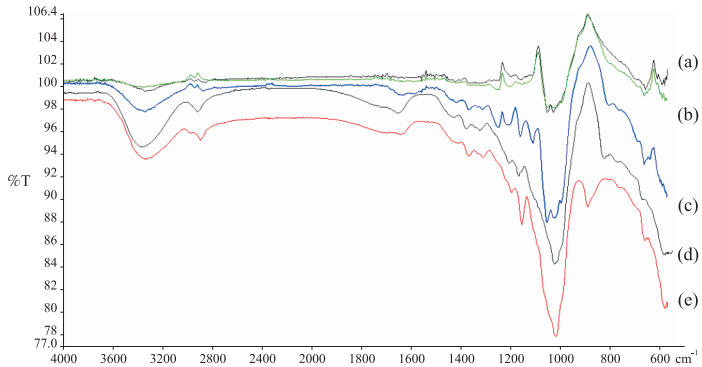

Fig. 3. FTIR spectra of cotton linter, and NCC specimens: (a) cotton linter, (b) RS50, (c) NCC55, (d) NCC50, and (e) NCC60.

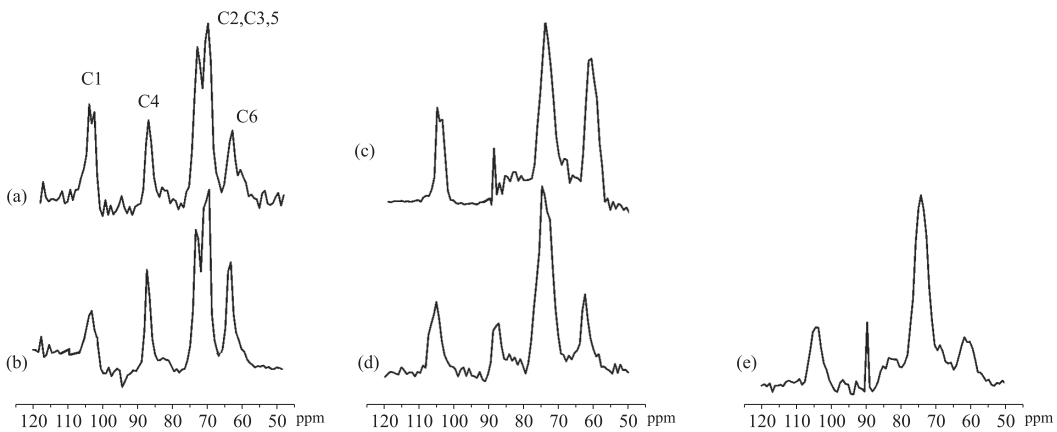

Fig. 4. The CP/MAS ^{13}CSNMR spectra of hydrolysis products: (a) cotton linter, (b) RS50, (c) NCC50, (d) NCC55, and (e) NCC60.

61.2. For NCC55, these were C1: 105.7, C2, 3, and 5: 75.4, C4: 89.8, and C6: 63.0. And for NCC60, these were C1: 105.0, C2, 3, and 5: 74.6, C4: 90.2, and C6: 60.6. Previous studies (Tomas et al. 2003, Wang et al. 2007) mentioned that sulfonic ester groups were mostly attached to the C6 and C2 positions of the glucose ring, and as a consequence, shifted the C6 position toward a lower magnetic domain (downfield region). But in our study, the C6 position moved from the original 65 ppm upfield, which may indicate a crystalline type change (Ago et al. 2004).

In Fig. 4, comparing the chemical shifts of cotton linter vs. the NCC specimens, only the C2 and C4 positions tended to shift downfield, which was thought to arise from the newly added sulfonic ester bonds (Tomas et al. 2003, Zhao et al. 2006). All NCC spectra also showed that C4 atoms shifted more than C1 atoms. This, according to Tomas et al. (2003), was because the positions of sulfonic ester bonds were mostly present at or near the non-reducing end of the cellulose chain, and rarely at the C1 position. This phenomenon implied that during sulfuric acid hydrolysis of cotton linter, the cellulosic chain was pared from the crystalline region by a unit of

cellubiose. Also, the sulfate esters bonds were found only on the surface of NCC without penetrating the interior.

Thermo-degradation behaviors

The thermal degradation parameters of the hydrolysis products are listed in Table 4. According to a previous study (Wang et al. 2007), the thermal stability of NCC significantly decreases due to the presence of residual sulfuric acid absorbed onto the cellulosic hydroxyl groups. In order to prevent this unexpected weight loss, the NCC specimens of our study were neutralized with sodium hydroxide. However, even with the removal of sulfate, the thermal degradation temperature of the NCCs was still lower than that of the cotton linter. The probable cause was that the large amounts of hydroxyl groups exposed with the increased specific surface areas were absorbing atmospheric moisture; and along with the rising temperature, sulfate ester bonds desorbed and reacted with the water molecules to create sulfuric acid, leading to structural damage to NCC and a reduction in the thermal degradation temperature (Wang et al. 2007, Rosa et al. 2010).

The DTG curves in Fig. 5 show that the degradation of NCC50 and NCC55 occurred within a wider temperature range and showed 2 well-separated pyrolysis processes in the DTG curves. For NCC50, the first pyrolysis step occurred at 150.0℃ and the second at 337.8℃. For NCC55, the first pyrolysis step, similar to NCC50, occurred at 146.4℃; however, the second degradation temperature was much lower than that of the NCC50, and occurred at 205.2℃. The thermal decomposition temperature of NCC60, on the other hand, had considerably shifted to a higher temperature, and occurred within a narrow temperature range at 243.1℃. Cotton linter and RS50 showed similar DTG curves with degradation temperatures beginning at ca. 300℃.

In order to explain our research results in detail, the TGA parameters must be discussed together with the FTIR and TEM results. Based on the literature review, the factors that influenced thermal degradation temperature include sample characteristics (such as sample size, stability of the functional groups, moisture content of samples, etc.), and experimental factors (for example, the heating rate, nitrogen flow rate, etc.) (Roman and Winter 2004). In our study, influences of the experimental factors could largely be eliminated, and the influence of sample moisture content was present only at temperatures below 100℃. As a consequence, only 2 factors of sample size and functional group stability might have impacted the TGA results. In general, the weight loss of a small sample is faster then that of a larger one. Thus, a sample with more-stable functional groups will have a higher thermal degradation temperature.

Comparing the results of Table 4 and Fig.

Table 4. Thermo-degradation parameters measured by TGA analysis for hydrolysis products produced under different conditions

Sample	Step 1		Step 2		Char at
	Onset temp (℃)	Weight loss (%)	Onset temp (℃)	Weight loss (%)	800℃ (%)
Cotton linter	300.4	53.0	-	-	8.9
RS50	289.2	55.5	-	-	7.4
NCC50	150.0	23.6	337.8	12.5	26.5
NCC55	146.4	10.0	205.2	60.9	15.0
NCC60	243.1	17.7	-	-	31.7

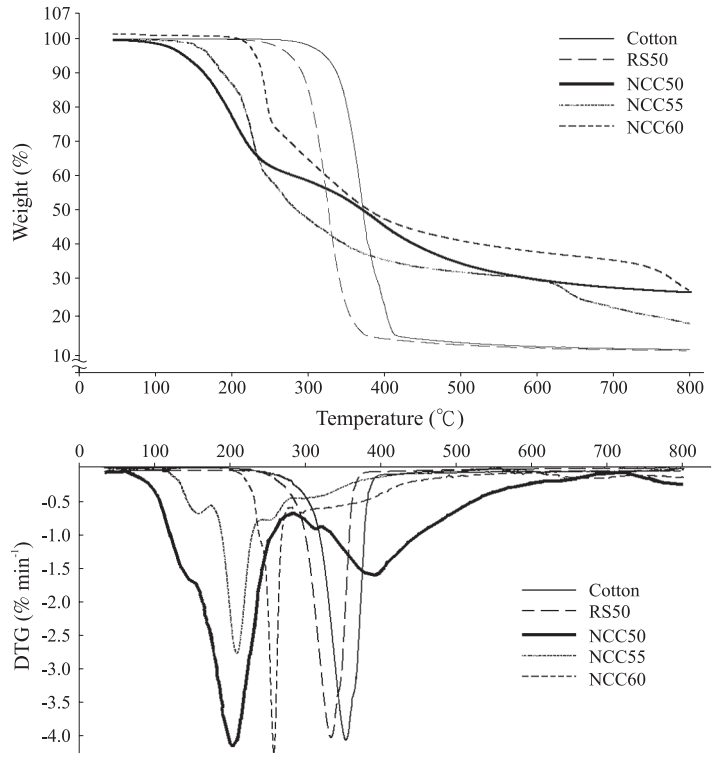

Fig. 5. Thermo-gravimetric (TG) and differential TG (DTG) curves of the hydrolysis products produced under different conditions.

3, for NCC50 and NCC55 with detectable sulfate ester groups, the first step of pyrolysis occurred at a lower temperature, which agrees well with a previous study (Kim et al. 2010). The second pyrolysis step of NCC55 showed greater weight loss and a lower temperature than those of NCC50, which may have been due to the NCC55 containing relatively more sulfate esters than did NCC50, and also the greater amorphous fraction presented by NCC55. According to the results of Kim et al. (2010), NCC of larger sizes would have higher thermal degradation temperatures. However, our results tended to disagree with their observations. The probable cause for the difference might be that they considered only sample sizes as a single variable, whereas our results were compounded with other factors. The reason that NCC60 had a lower thermal degradation temperature then NCC50 was because it had more-corroded crystalline regions and smaller diameters, as can be noted in Fig. 2 and Table 3.

Based on our results, we hypothesized that the sulfate ester bonds formed by sulfuric acid were mostly present on the surface, and the disrupted lattices of the NCC specimens, which were easily detached from the surfaces, re-formed sulfuric acid, dissolved the disordered amorphous fraction, and entered some crystalline regions causing partial degradation of cellulose crystallites with rising temperatures. Based on this hypothetical model, we can provide reasonable explanations for the fact that even though NCC55 had a higher crystallinity than NCC60, it nevertheless had

a lower second-step thermal degradation temperature than the latter did.

The hypothetical pathway of sulfuric acid hydrolysis

Sulfuric acid hydrolysis of cellulose is a complex heterogeneous reaction, which involves different physical factors and hydrolytic chemical reactions. A slight modification of the experimental conditions could have resulted in varying pathways and products. Some previous studies pointed out that the permeability of different sulfuric acid concentrations often cause significant variations in NCC morphology, thermal degradation behaviors, and crystallinity (Xiang et al. 2003, Mohamed and Hassan 2007). Xiang et al. (2003) suggested that the first step of cellulose acid hydrolysis is penetration of the acid into the cellulose matrix. The process is a first-order reaction which follows the rule of the Arrehnius equation: $k_i = k_{io} \times A^{mi} \times e^{-\frac{E_i}{RT}}$, where k_{io} is the pre-exponential factor, A is the concentration of the acid, m_i is an exponent indicating the acid's effect, and E_i is the activation energy. Thus, if sulfuric acid of a specific concentration is capable of totally penetrating into the cellulosic matrix, then it is capable of quickly hydrolyzing it. Hydrolysis, as the name implies, needs to add water molecules to the reactant in the reaction. Thus, too high an acid concentration might not provide enough water; whereas too low an acid concentration might not have sufficient penetrating power. Effective working sulfuric acid concentrations need to carefully be selected. Based on our research data, the hypothetical pathway is depicted in Fig. 6.

By comparing the morphology of NCC specimens shown in Fig. 2, it is plausible that a relatively weak sulfuric acid concentration (i.e., 50%), could not effectively penetrate into the interior of the cotton linter, and the

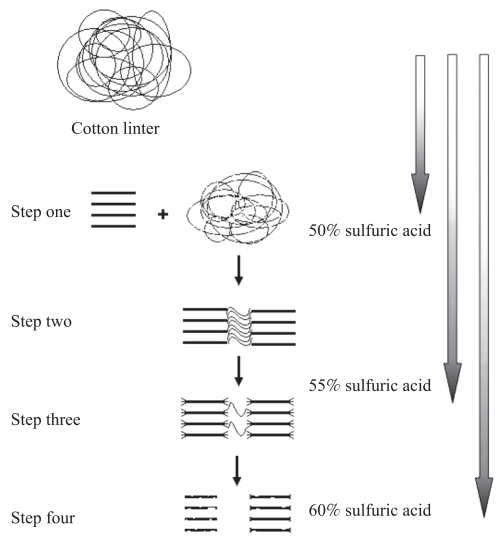

Fig. 6. Hypothetical pathway of sulfuric acid hydrolysis.

chemical reaction primarily entailed paring the outer portions of the fiber into spherical particles. When we observed the performance of 55 and 60% sulfuric acid in hydrolyzing cotton linter, notably only 2 min after mixing with the cotton linter, the liquid phase turned clear and no residue was present after centrifugation. Meanwhile, the liquid phase of the 50% sulfuric acid/cotton linter mixtures remained milky white, indicating a weak infiltration of the acid and the presence of large, visible particles. By comparing Table 3 and Fig. 2, we noted that NCC55 had a greater aspect ratio than did NCC50 and NCC60, as well as larger crystallite length and width. Hence, we assumed that 55% sulfuric acid had sufficient penetrating power and upon contacting cotton linter would first dissolve the outer layers and then penetrate into the amorphous regions in the interior and even begin to disrupt the crystalline regions until being quenched by acid neutralization. In the meantime, the external NCC was further hydrolyzed into sugars and other acid derivatives. From Fig. 2, we can discern that in

addition to what occurred with the 55% acid, the 60% acid penetrated even deeper into the crystallites and created a more-fragmented product with smaller particle diameters than the cellulose element fibers (Stephanie et al. 2005). However, whether the 2 acid concentrations can totally dissolve the amorphous regions and how disruptive they were to the crystalline regions must await further studies.

CONCLUSIONS

Our experimental design indicated that the solid/liquid ratio contributed less to hydrolysis than did other factors. For future cost savings, a lower ratio could be employed with minor consequences. The results also indicated that NCC specimens produced from different acid-hydrolysis conditions presented variable physical characteristics, but all had narrow size distribution ranges. The morphology of the NCC specimens suggested that a 55% sulfuric acid hydrolysis condition produced nanocrystallines with a suitable aspect ratio which were adequate reinforcing materials to produce polymer composites. However, their thermal degradation behavior might be a matter of concern. On the other hand, those NCC specimens with lower aspect ratios might be suitable for modifying the surface properties of polymer composites incorporating them, or be applied as medicinal additives. Quantities of the hydroxyl and sulfate esters groups greatly increased along with sulfuric acid hydrolysis. For future studies, those active functional groups, especially the ones on the C2 and C4 positions, can be further modified for different purposes to more fully explore applications of NCC.

ACKNOWLEDGMENTS

Ms. Irene Chen and the staff of the Division of Wood Cellulose, Taiwan Forestry Research Institute provided irreplaceable assistance and instrumental help. We hereby gratefully acknowledge their contributions.

LITERATURE CITED

Ago M, Endo T, Hirotsu T. 2004. Crystalline transformation of native cellulose from cellulose *I* to cellulose *II* polymorph by a ball-milling method with a specific amount of water. Cellulose 11:163-7.

Kim UJ, Eomb SH, Wada M. 2010. Thermal decomposition of native cellulose: influence on crystallite size. Polym Degrad Stab. (in press).

Kuo CH, Lee CK. 2009. Enhancement of enzymatic saccharification of cellulose by cellulose dissolution pretreatments. Carbohydr Polym 77:41-6.

Lin CH, Conner AH, Hill CC. 1991. The heterogeneous character of the dilute acid hydrolysis of crystalline cellulose. II. hydrolysis in sulfuric acid. J Appl Polym Sci (42):417-26.

Mohamed E, Hassan ML. 2007. Physical and mechanical properties of microcrystalline cellulose prepared from agricultural residues. Carbohydr Polym 67:1-10.

Morán JI, Alvarez VA, Cyras VP, Vázquez A. 2008. Extraction of cellulose and preparation of nanocellulose from sisal fibers. Cellulose 15:149-59.

Roman M, Winter WT. 2004. Effect of sulfate groups from sulfuric acid hydrolysis on the thermal degradation behavior of bacterial cellulose. Biomacromolecules 5:1671-7.

Rosa MF, et al. 2010. Cellulose nanowhiskers from coconut husk fibers: effect of preparation conditions on their thermal and morphological behavior. Carbohyd Polym (in press).

Stenius P, Andresen M. 2009. Preparation, properties and chemical modification of nano-sized cellulose fibrils. In: Platikanov D, Exerowa D, editors. Highlights in colloid science.

Weinheim, Germany: Willey-Vch Verlag. p 135-53.

Stephanie BC, Roman M, Gray DG. 2005 Effect of reaction conditions on the properties and behavior of wood cellulose nanocrystal suspensions. Biomacromolecules 6(2):1048-54.

Sun JX, Xu F, Sun XF, Xiao B, Sun RC. 2005. Physico-chemical and thermal characterization of cellulose from barley straw. Polym Degrad Stab 88:521-31.

Thomas M, Chauvelon G, Lahaye M, Saulnier L. 2003. Location of sulfate groups on sulfo-acetate derivatives of cellulose. Carbohydr Res 338:761-70.

Vandyke RH, Staud CJ, Gray HL. 1931. Treatment of cellulose and oxidized cellulose with acetic-sulfuric acid mixtures. J Am Chem Soc 53:2725-32.

Wang N, Ding NY, Cheng RS. 2007. Thermal degradation behaviors of spherical cellulose nanocrystals with sulfate groups. Polymer 48: 3486-93.

Wong SS, Kasapis S, Tan YM. 2009. Bacterial and plant cellulose modification using ultrasound irradiation. Carbohydr Polym 77:280-7.

Xiang Q, LEE YY, Petterssom PO, Torget RW. 2003. Heterogeneous aspects of acid hydrolysis of α-cellulose. Appl Biochem Biotechnol 3:105-8.

Yang ZP, Xu SW, Ma XL, Wang SY. 2008. Characterization and acetylation behavior of bamboo pulp. Wood Sci Technol 42:621-32.

Zhang JG, Jiang N, Dang Z, Elder TJ, Ranauskas AJ. 2008. Oxidation and sulfonation of cellulosics. Cellulose15:489-96.

Zhang J, Luo J, Tong DM, Zhu LF, Dong LL, Hu CW. 2010. The dependence of pyrolysis behavior on the crystal state of cellulose. Carbohydr Polym 79:164-9.

Zhao HB, Kwak JH, Zhang ZC, Brown HM, Arey BW, Holladay JE. 2006. Studying cellulose fiber structure by SEM, XRD, NMR and acid hydrolysis. Carbohydr Polym 68:235-41.